The air object tracking in 3D space using distance measurements

Tomasz Kraszewski*, Grzegorz Czopik
Military Academy of Technology, Faculty of Electronics, Radioelectronics Institute,
00–908 Warsaw 46, gen. Sylwester Kaliski 2 St.

ABSTRACT

The widespread availability of global navigation satellite signals has become so obvious that it is difficult to imagine their absence. However, under conditions of severe intentional interference, these signals can be degraded (*spoofing*) or blocked (*jamming*). It becomes necessary to search for solutions that allow to create your own location system operating in the local coordinate system. The ultrawideband modules that measure distances (that are on the institute's equipment) can be used for this purpose. Therefore, an attempt was made to analyze algorithms based on the measurement of this parameter that allow the location and tracking of the air objects (drone) in 3D space. Although the use of radio waves is also assumed here, the spectrum of the signal is dispersed. This allows you to avoid detecting signals and thereby avoiding interference. The adopted method also gives potential opportunities to build an indoor positioning system where satellite system signals are unavailable. Studies have been carried out for various air object trajectories in open space. They were analysed using the ordinary least squares method, the extended Kalman filter and its modification. Graphic imagery of trajectory and calculated values of traced trajectory errors for different system configurations are shown. On this basis, the implemented algorithms were evaluated.

Keywords: tracking, Kalman filter, localization, ultra-wideband technology.

1. INTRODUCTION

In various applications, both unmanned systems for military[10] and civil[12] purposes, it is very useful to obtain a precise location of the object in three-dimensional space in a specific area of interest. The creation of a local coordinate system for such operations using unmanned aerial vehicles (UAVs), commonly known as drones, can be considered unnecessary and difficult to justify. The ubiquitous and cheap global navigation satellite system (GNSS) receivers and the widespread and continuous availability of satellite signals allow to determine the exact position at almost every point of the globe 24 hours a day. However, this obvious and useful positioning capability can be lost in conditions of intentional interference. The frequencies and structures of the radio signals on which they operate are widely known. These signals can be degraded (*spoofing*) by "placing" false signals or blocked (*jamming*) by using high-power jamming devices covering appropriate electromagnetic emissions.

An attempt to create a system that would allow the definition of a local coordinate system was made at the Institute of Radioelectronics. Also here it is assumed to use radio waves, but the signal structures used will have enough dispersed spectrum that their detection for possible later interference will be much more difficult or even impossible. These conditions are met by ultrawideband modules (UWB)[3,6] working with signals in this technology.

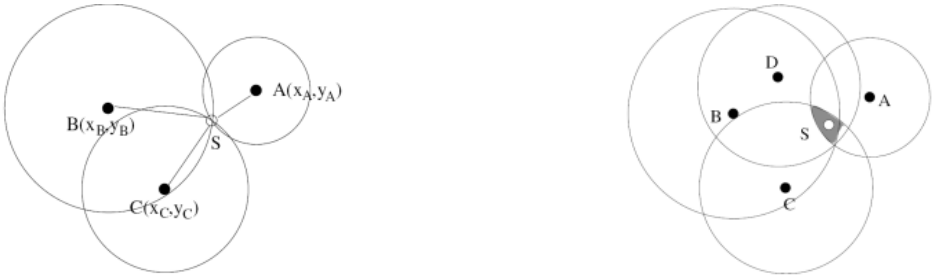

Figure 1. The positioning system using distance measurement: trilateration (left) and multilateration (right)[13]

* tomasz.kraszewski@wat.edu.pl; phone +48 261 83 7071; www.wat.edu.pl

Radioelectronic Systems Conference 2019, edited by Piotr Kaniewski, Jan Matuszewski, Proc. of SPIE
Vol. 11442, 1144210 · © 2020 SPIE · CCC code: 0277-786X/20/$21 · doi: 10.1117/12.2565281

It is also planned to examine the proposed solution for the construction of an indoor positioning system where satellite system signals are not available.

Because the ultrawideband modules used measure the distance (by measuring the signal propagation time between any two modules), it was decided to analyze algorithms that allow the location and tracking of the object in 3D space based on the measurement of this parameter.

The system using distance (time) measurement from the point of view of the position line shape is a circular system. The measured distance in 2D space defines circles with a radius value corresponding to the measured distance (Fig.1), while in 3D space we are dealing with spheres with a fixed distance value (Fig.2)[3,8]. In the first case, to determine the location of the object, a sufficient number of measurements is three (*trilateration*), but if we want to estimate the height also then we need to use at least four modules (*multilateration*). The estimated location point in ideal conditions would be the intersection of circles / spheres. However, real conditions cause measurement disturbances, resulting in an error of determining the location.

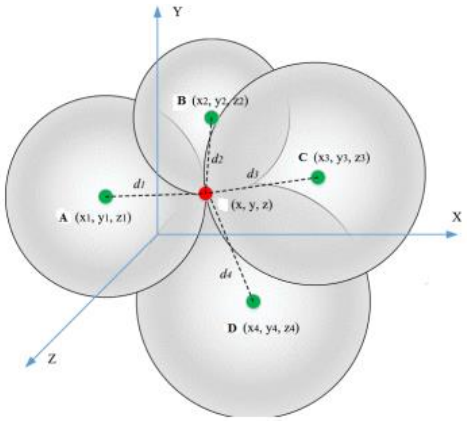

Figure 2. The principle of location in 3D space in circular system[3]

The first part presents methods of estimating the air object position (drone) in 3D space in a system using UWB modules measuring distances.

Further, simulation tests were carried out assuming several trajectories of the localized object's movement. The system properties with various module configurations (location and height) were also analysed. All these implementations will form the basis for further stages of research in real conditions. For this reason, the configurations of the generated trajectories (range of changes in object location value) were determined by the future potential testing area in real conditions at the Military University of Technology (MUT) training area (Fig.3).

The last part presents the analysed ideal and estimated trajectories as well as the values of calculated position errors.

Figure 3. The perpendicular projection of trajectory I onto the XY plane against the background of the MUT training area

2. LOCATION ESTIMATION METHODS OF THE AIR OBJECT

The results of the air object trajectory tracking studies presented below are based on two methods of the parameter value estimation (explained variable) based on the data value of the observed variable.

In the further part of the study, two methods are approximated: ordinary least squares – OLS[2,4,8] (estimating the coordinates of a single trajectory point separately for each point without tracking function) and algorithms that track object trajectory using extended Kalman filtration – EKF[1,3,6].

2.1 OLS – general case

The statistical approach to trilateration (multilateration) leads to the solution of the nonlinear least squares problem (NLS). One common approach to solve this problem is the linearization of nonlinear function. Given this approach, the linear location methodology attempts to transform nonlinear expressions into a set of the linear equations (1) with zero mean interference[2,4,8].

$$y = \beta_0 + \beta_1 x_1 + \cdots + \beta_k x_k + \varepsilon \tag{1}$$

Such a system of linear equations can be written in matrix form as:

$$\boldsymbol{y} = \boldsymbol{X}\,\boldsymbol{\beta} + \boldsymbol{\varepsilon} \tag{2}$$

where the sizes of individual matrices and vectors: $\boldsymbol{y} \to n \times 1$; $\boldsymbol{X} \to n \times (k+1)$; $\boldsymbol{\beta} \to (k+1) \times 1$; $\boldsymbol{\varepsilon} \to n \times 1$; k – number of explained variables; n – number of observations (measurements), $\boldsymbol{\varepsilon}$ – random component. Later, β means the true (unknown) value of the parameter vector, and, a $\hat{\beta}$ its estimation result.

The $\boldsymbol{y}$ vector is the observed (empirical) value of the explained variable, and $\widehat{\boldsymbol{y}}$ is the theoretical value resulting from estimates:

$$\widehat{\boldsymbol{y}} = \boldsymbol{X}\,\widehat{\boldsymbol{\beta}} \tag{3}$$

The vector of residuals $\boldsymbol{e}$ is given by:

$$\boldsymbol{e} = \boldsymbol{y} - \widehat{\boldsymbol{y}} = \boldsymbol{y} - \boldsymbol{X} * \widehat{\boldsymbol{\beta}} \tag{4}$$

If the studied phenomenon can be described with a model (2), then unknown parameters can be obtained using the ordinary least squares method. The idea of this method is to find such values of an unknown parameter vector $\boldsymbol{\beta}$ that minimize the sum of squares of residuals, i.e. differences between the observed and theoretical values:

$$\widehat{\boldsymbol{\beta}}^{OLS} = \arg\min_{\boldsymbol{\beta}} \boldsymbol{e}^T \boldsymbol{e} \tag{5}$$

The sum of squared residuals (SSE) as a function of the searched parameter vector $\boldsymbol{\beta}$ is $\boldsymbol{e}^T\boldsymbol{e}$:

$$SSE(\beta) = \boldsymbol{e}^T\boldsymbol{e} = (\boldsymbol{y} - \widehat{\boldsymbol{y}})^T(\boldsymbol{y} - \widehat{\boldsymbol{y}}) = (\boldsymbol{y} - \boldsymbol{X}\,\boldsymbol{\beta})^T(\boldsymbol{y} - \boldsymbol{X}\,\boldsymbol{\beta}) \tag{6}$$

$$SSE(\beta) = \boldsymbol{y}\,\boldsymbol{y}^T - 2\,\boldsymbol{y}^T\boldsymbol{X}\,\boldsymbol{\beta} + \boldsymbol{\beta}^T\,\boldsymbol{X}\,\boldsymbol{X}\,\beta \tag{7}$$

To find the $\widehat{\boldsymbol{\beta}}$ that minimizes the sum of squared residuals, we need to take the derivative of (7) with respect to $\widehat{\boldsymbol{\beta}}$. This gives us the following equation:

$$\frac{\partial SSE(\boldsymbol{\beta})}{\partial \boldsymbol{\beta}} = -2\,\boldsymbol{X}^T\boldsymbol{y} + 2\,\boldsymbol{X}^T\boldsymbol{X}\,\boldsymbol{\beta} \tag{8}$$

Comparing the first derivative, i.e. (8) to zero, we what are called the normal equations:

$$\boldsymbol{X}^T\boldsymbol{y} = \boldsymbol{X}^{\,T}\,\boldsymbol{X}\,\boldsymbol{\beta} \tag{9}$$

Finally transforming (9) we get the expression describing the OLS method:

$$\widehat{\boldsymbol{\beta}}^{OLS} = (\boldsymbol{X}^T\boldsymbol{X})^{-1}\boldsymbol{X}^T\boldsymbol{y} \tag{10}$$

2.2 OLS – case study

For a specific analyzed case of tracking the location of an air object in 3D space, formula (10) takes the following form:

$$d\boldsymbol{P} = (\boldsymbol{H}^T\boldsymbol{H})^{-1}\boldsymbol{H}^T d\boldsymbol{R} \tag{11}$$

The individual matrices and vectors for the OLS method have the following forms: $d\boldsymbol{P}$ – position correction vector for individual object coordinates:

$$d\boldsymbol{P} = [dx \quad dy \quad dz]^T \tag{12}$$

and matrix $\boldsymbol{H}$:

$$\boldsymbol{H} = \begin{bmatrix} \frac{\partial R_1}{\partial x} & \frac{\partial R_1}{\partial y} & \frac{\partial R_1}{\partial z} \\ \frac{\partial R_2}{\partial x} & \frac{\partial R_2}{\partial y} & \frac{\partial R_2}{\partial z} \\ \frac{\partial R_3}{\partial x} & \frac{\partial R_3}{\partial y} & \frac{\partial R_3}{\partial z} \\ \frac{\partial R_4}{\partial x} & \frac{\partial R_4}{\partial y} & \frac{\partial R_4}{\partial z} \end{bmatrix} = \begin{bmatrix} \frac{\hat{x}_{k-1}-x_{m1}}{R_1} & \frac{\hat{y}_{k-1}-y_{m1}}{R_1} & \frac{\hat{z}_{k-1}-z_{m1}}{R_1} \\ \vdots & \vdots & \vdots \\ \frac{\hat{x}_{k-1}-x_{m4}}{R_4} & \frac{\hat{y}_{k-1}-y_{m4}}{R_4} & \frac{\hat{z}_{k-1}-z_{m4}}{R_4} \end{bmatrix} \tag{13}$$

where: k – discrete time index, R_i – distance between i – *th* modul and the localized object at the moment $k-1$, $\hat{x}, \hat{y}, \hat{z}$ – estimated coordinates values of the tracked object, x_{mi}, y_{mi}, z_{mi} – coordinate values of i – *th* module.

In order to determine the best position estimate, the location correction vector of the tracked object was calculated (11). The elements of the $d\boldsymbol{R}$ vector correspond to subsequent differences between the measured values of the distance between and i – *th* module and the tracked object, and their estimated values:

$$d\boldsymbol{R} = [d\boldsymbol{R}_1 \quad d\boldsymbol{R}_2 \quad d\boldsymbol{R}_3 \quad d\boldsymbol{R}_4]^T \tag{14}$$

The $d\boldsymbol{P}$ correction vector represents the estimation error of the object's position parameters, therefore it is added to the current estimate and an iterative attempt to minimize its value is made:

$$\widehat{\boldsymbol{P}}_{k+1} = \widehat{\boldsymbol{P}}_k + d\boldsymbol{P} \tag{15}$$

The iteration shall be terminated when the following condition is met:

$$|d\boldsymbol{P}| \leq epsilon \tag{16}$$

where: $epsilon$ – assumed accuracy of position correction.

The advantage of this algorithm is the low mathematical complexity. On the other hand, it needs the appropriate selection of the starting point for the object position, several iterations in order to obtain an precise estimate of parameters and appropriate geospatial configuration of the modules.

2.3 EKF

Kalman filtration is widely well known so in the further part of the study only the elements necessary to describe and analyse the presented system will be cited.

The operation of each Kalman filtration algorithm is based on the estimation of a new process state in two consecutive steps[1,3,5,7]: Prediction – the current process status is estimated based on the information from the previous step without taking into account any measurements and Correction – involves the use of new real measurements (noised) to correct the values determined in the previous step, at the prediction stage.

Regardless of the type of filter, its operation scheme (Fig.4) can be presented in the form of several operations[1,5]: initialization performed once at the beginning of the filter operation ($\boldsymbol{x_0}$,$\boldsymbol{P}_0$), and then recursively: prediction of the state vector ($\boldsymbol{x}$) and the covariance matrix of prediction errors ($\boldsymbol{P}$), calculation of Kalman's gain matrix ($\boldsymbol{K}_{k+1}$) and correction of prediction results using the last current measurement[3,6,9].

When developing the tracking system using Kalman filtration, it is necessary to define the state (dynamics) (Eq.17) and observation (Eq.18) equations. Often, it turns out that one or both of them have a non-linear nature and then it is necessary to use a non-linear filtration algorithm.

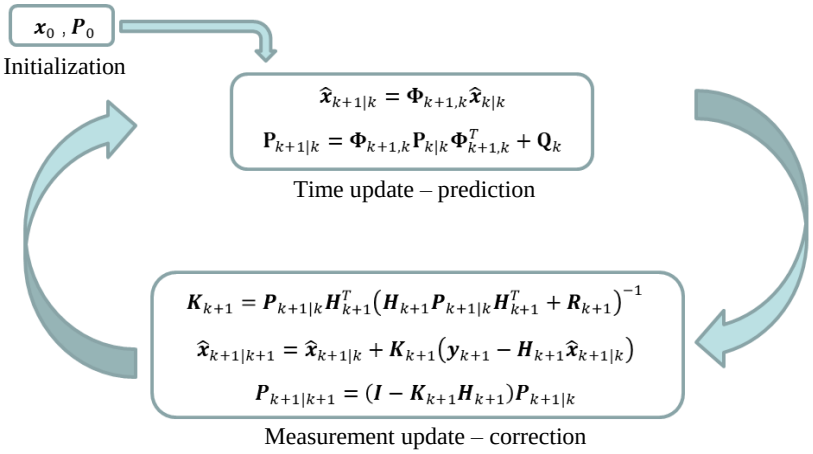

Figure 4. The Kalman filtration process[9] – block diagram

In the system under consideration, it is assumed that both measurement errors ($\boldsymbol{v}$) and process interferences ($\boldsymbol{w}$) are Gaussian noises (taken into account at a later stage by the appropriate $\boldsymbol{Q}_k$ and $\boldsymbol{R}_{k+1}$ matrices). The discreet version of the system model consists of the dynamics and observation equations[1,7]:

$$\boldsymbol{x}_{k+1} = \boldsymbol{f}(\boldsymbol{x}_k) + \boldsymbol{w}_k \tag{17}$$

$$\boldsymbol{z}_{k+1} = \boldsymbol{h}(\boldsymbol{x}_{k+1}) + \boldsymbol{v}_{k+1} \tag{18}$$

Matrices $\boldsymbol{\Phi}$ and $\boldsymbol{H}$ (transition and observation) are Jacobi matrices composed of partial derivatives of the nonlinear $\boldsymbol{f}$ and $\boldsymbol{h}$ functions with respect to all elements of the state vector.

$$\boldsymbol{\Phi}_{k+1,k} = \frac{\partial \boldsymbol{f}}{\partial \boldsymbol{x}}|_{\boldsymbol{x}=\hat{\boldsymbol{x}}_{k|k}} \qquad \boldsymbol{H}_{k+1} = \frac{\partial \boldsymbol{h}}{\partial \boldsymbol{x}}|_{\boldsymbol{x}=\hat{\boldsymbol{x}}_{k+1|k}} \tag{19}$$

In the case under consideration, we achieve the linear equation of system dynamics (state) and a non-linear equation of observation[1,7]:

$$\boldsymbol{x}_{k+1} = \boldsymbol{\Phi}_{k+1,k}\mathbf{x}_k + \mathbf{w}_k \tag{20}$$

$$\boldsymbol{z}_{k+1} = \boldsymbol{h}(\boldsymbol{x}_{k+1}) + \boldsymbol{v}_{k+1} \tag{21}$$

therefore it is only necessary to calculation the **H** matrix as partial derivatives.

The dynamics model adopted in the research looks as follows:

$$\begin{bmatrix} x \\ v_x \\ y \\ v_y \\ z \\ v_z \end{bmatrix}_{k+1} = \begin{bmatrix} \boldsymbol{\Phi}_x & 0_{2x2} & 0_{2x2} \\ 0_{2x2} & \boldsymbol{\Phi}_y & 0_{2x2} \\ 0_{2x2} & 0_{2x2} & \boldsymbol{\Phi}_z \end{bmatrix} \begin{bmatrix} x \\ v_x \\ y \\ v_y \\ z \\ v_z \end{bmatrix}_k + \begin{bmatrix} w_x \\ w_{vx} \\ w_y \\ w_{vy} \\ w_z \\ w_{vz} \end{bmatrix}_k \tag{22}$$

$$\boldsymbol{\Phi}_x = \boldsymbol{\Phi}_y = \boldsymbol{\Phi}_z = \begin{bmatrix} 1 & T \\ 0 & 1 \end{bmatrix} \tag{23}$$

where: x, y, z – object coordinates in rectangular coordinate system, v_x, v_y, v_z – object velocity in rectangular coordinate system, w_x , w_{vx} , w_y , w_{vy}, w_z , w_{vz} – random disturbances of the motion model, T – discretization time.

The observation model[2,6], on the other hand, is the relationship between the measured distances in the system and the coordinates of the air object location in the state vector:

$$R_{j,i} = \sqrt{\left(X_i - x_j\right)^2 + \left(Y_i - y_j\right)^2 + \left(Z_i - z_j\right)^2} + v_j \tag{24}$$

where: R – measured distance between the *i-th* module and the located object, X_i, Y_i, Z_i – coordinates of the *i-th* module, x_j, y_j, z_j – coordinates of the *j-th* point of the analysed trajectory.

3. TESTING TRACKING ALGORITHMS

3.1 Research organization

Simulation studies of the air object location system were carried out using UWB modules measuring distance. The configuration of the modules placement corresponds to the possibility of placing them in the MUT training area (Fig. 3) at a later time.

The tests were carried out for different configurations of the deployment and installation height of individual modules (installation in a short time in a simple way for high system mobility) and various trajectories of the air object movement.

The images presented later show: trajectory I (with a shape similar to the number eight) and trajectory II (showing the movement of the object outside the area covered by the system placement).

Table 1. The position configuration of ultrawideband modules in 3D space.

Module number →		1	2	3	4
Coordinates ↓					
	X [m]	50	150	200	0
	Y [m]	0	0	70	70
Configuration 1 – C1	Z_1 [m]	0.2	0.2	0.2	0.2
Configuration 2 – C2	Z_2 [m]	1.2	1.2	0.2	0.2
Configuration 3 – C3	Z_3 [m]	1.2	0.2	1.2	0.2
Configuration 4 – C4	Z_4 [m]	0.2	2.2	2.2	0.2

In further analysis of distance data, the ordinary least squares method – OLS (as a reference algorithm), a tracking algorithm using extended Kalman filtration – EKF and its modification were used for the location of the object. This modification consisted of filter initialization with data from the approximation of the first trajectory point obtained using the OLS (EKF_{OLS}) algorithm.

3.2 Tests results – graphic imaging

The tests were carried out for two types of trajectories generated simulation in the Matlab® environment. Graphic images of the constant measured distance spheres for a circular system and their projections on the XY plane were presented for them. Then the ideal and estimated (using the OLS, EKF and EKF_{OLS} algorithms) trajectories were presented, as well as the estimated values of individual coordinates of the tracked air object. All these views are used to analyze the operation of the methods used to track the air object.

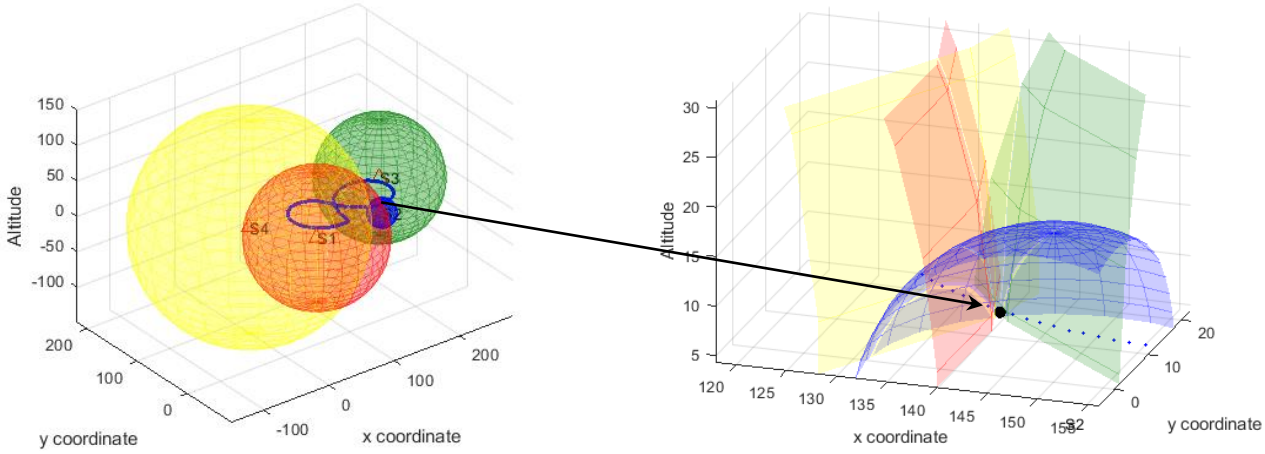

Figure 5. The spheres of equal distance circular system for each modules and trajectory I : 3D view (left) and zoom with the exemplary point of the estimated position (right)

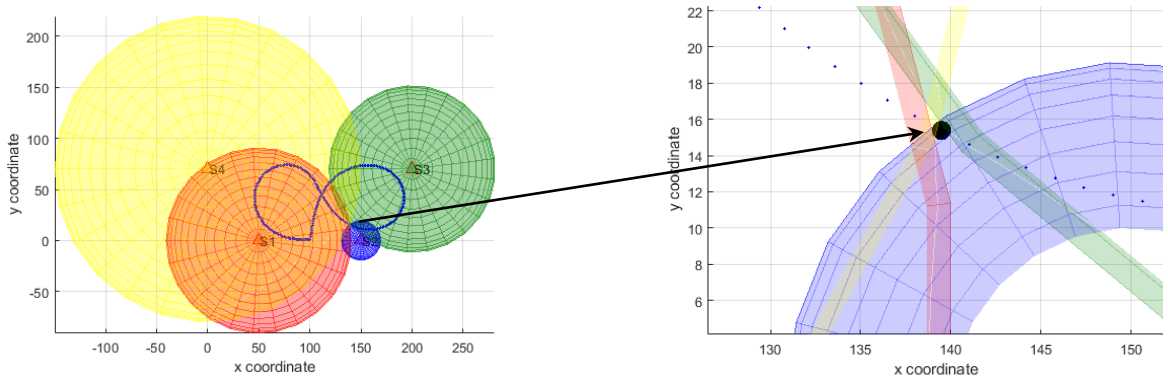

Figure 6. The spheres of equal distance circular system for each modules and trajectory I: projection view on the XY plane (left) and zoom with the exemplary point of the estimated position (right)

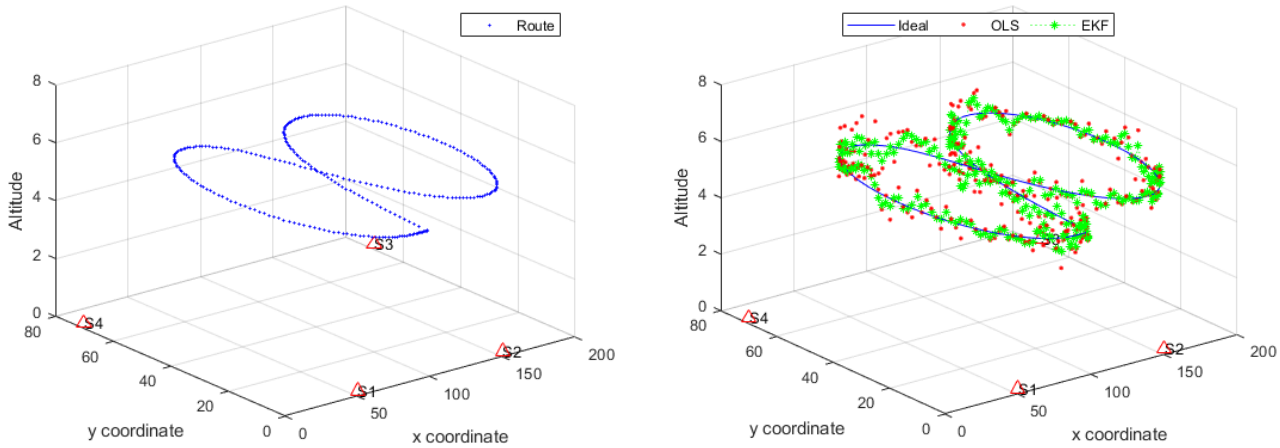

Figure 7. Trajectory I: ideal (blue), OLS estimated (red) and EKF estimated (green)

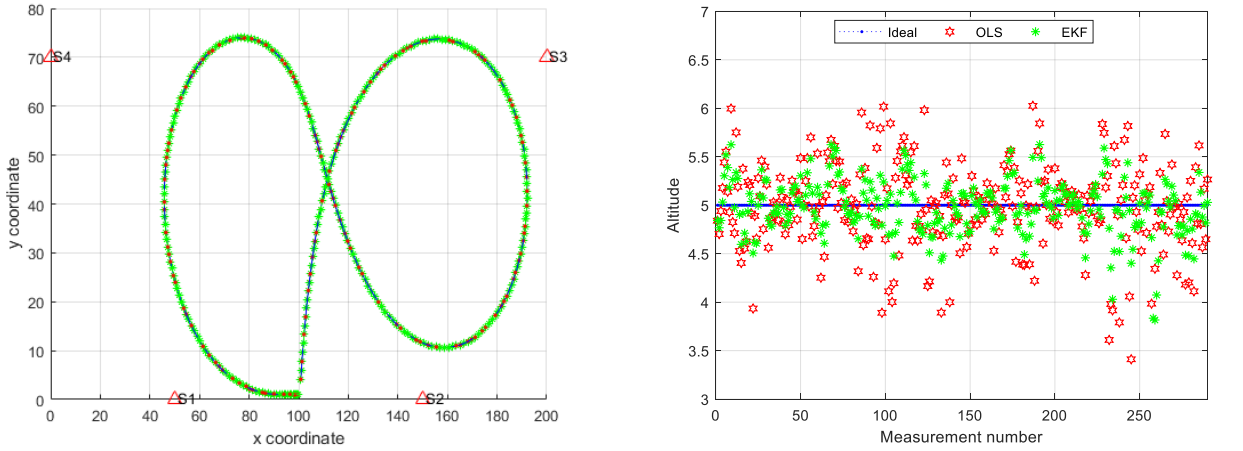

Figure 8. Trajectory I: projection view on the XY plane (left) and subsequent values of the estimated height of the object (right)

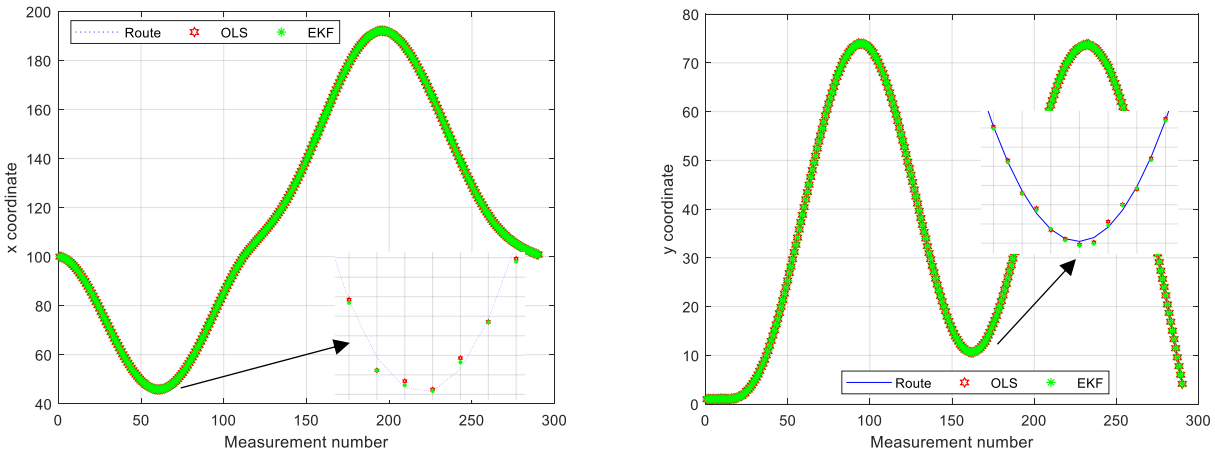

Figure 9. Trajectory I: subsequent estimated values of the X coordinate (left) and subsequent estimated values of the Y coordinate (right)

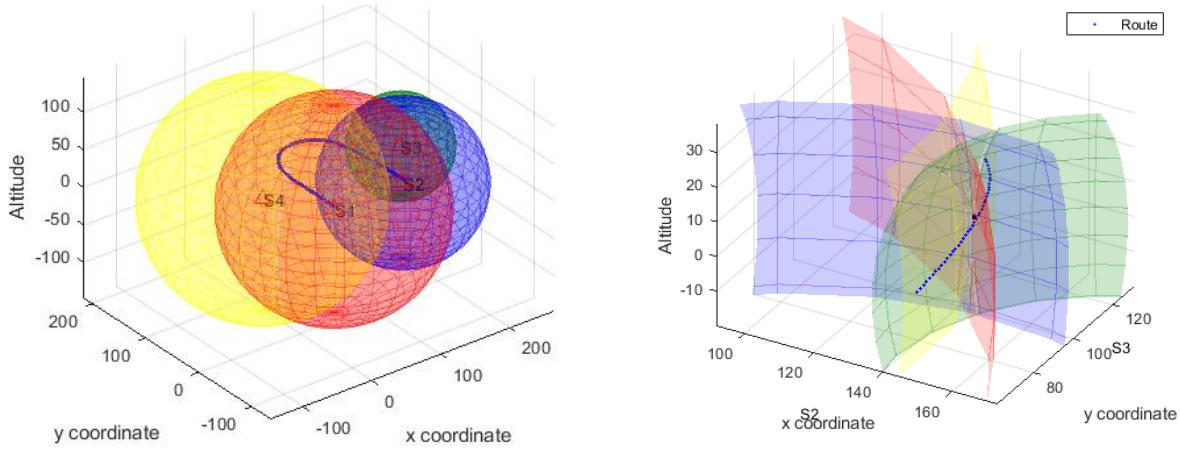

Figure 10. The spheres of equal distance circular system for each modules and trajectory II: 3D view (left) and zoom with the exemplary point of the estimated position (right)

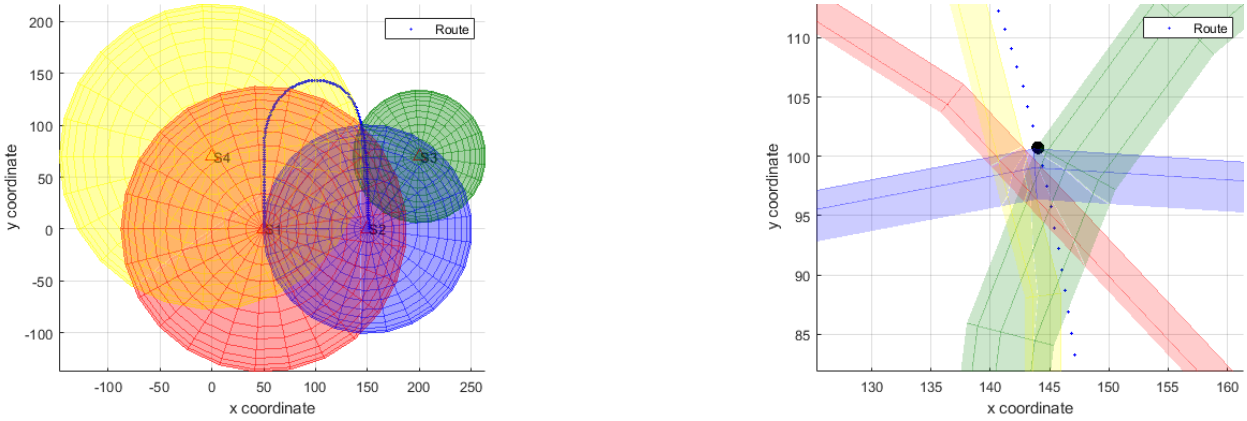

Figure 11. The spheres of equal distance circular system for each modules and trajectory II: projection view on the XY plane (left) and zoom with the exemplary point of the estimated position (right)

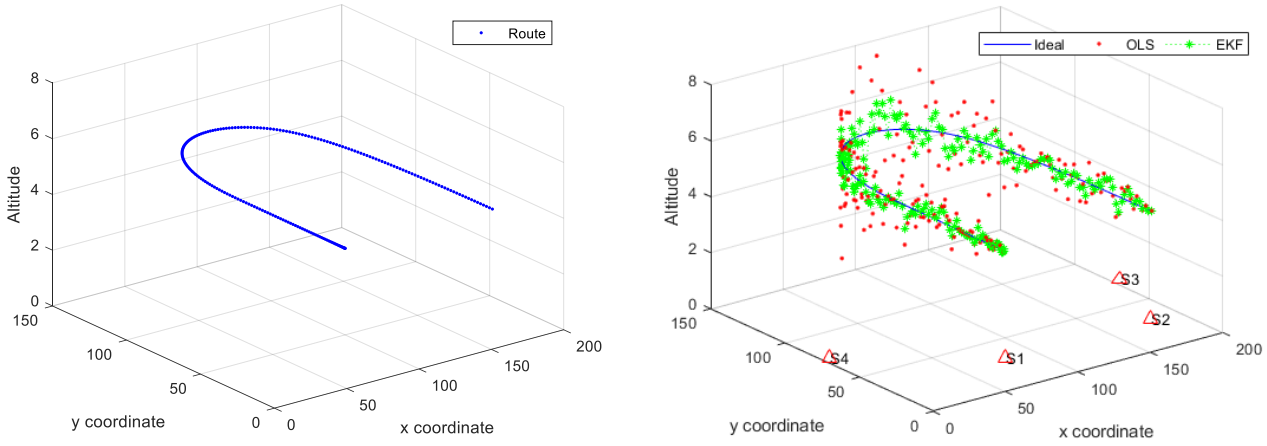

Figure 12. Trajectory II: ideal (blue), OLS estimated (red) and EKF estimated (green)

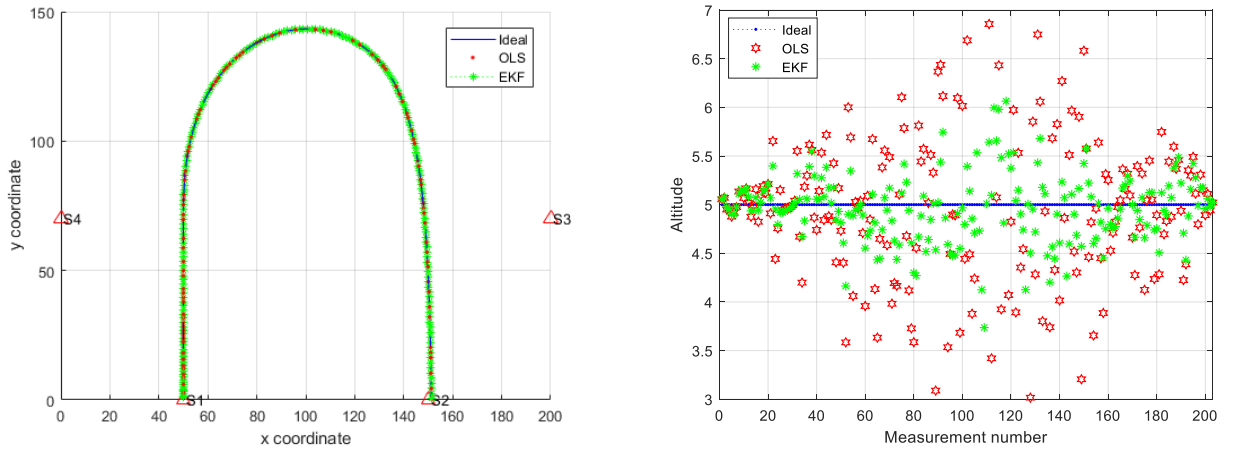

Figure 13. Trajectory II: projection view on the XY plane (left) and subsequent values of the estimated height of the object (right)

3.3 Tests results – validation

In order to verify the implementation of each algorithms[8,11], depending on the type of air object trajectory (moving inside or outside the system's operating area) and spatial configuration of the modules (changes in the position and height of mounting the modules), a quantitative assessment was also made using two types of statistical metrics[3,4]: root mean square error (25) and mean absolute error (26) of the estimated spatial location of the tracked air object:

$$RMSE_{Alg,l} = \left(\sum_{j=1}^{NoP}\sqrt{\left(x_j - x_{Alg,j}\right)^2 + \left(y_j - y_{Alg,j}\right)^2 + \left(z_j - z_{Alg,j}\right)^2}\right)/NoP \tag{25}$$

$$RMSE_{Alg} = \left(\sum_{l=1}^{NoR} RMSE_{Alg,l}\right)/NoR \tag{26}$$

where: l – implementation number; Alg – type of algorithm (OLS, EKF lub EKF_{OLS}); NoP – Number of Points, j – *j-th* point trajectory, $\boldsymbol{x}_j, \boldsymbol{y}_j, \boldsymbol{z}_j$ – ideal coordinates, $\boldsymbol{x}_{Alg,j}, \boldsymbol{y}_{Alg,j}, \boldsymbol{z}_{Alg,j}$ – coordinates estimated in the selected algorithm, NoR – Number of Realizations.

$$MAE_{Alg,l} = \sum_{j=1}^{NoP}\left(\left|x_j - x_{Alg,j}\right| + \left|y_j - y_{Alg,j}\right| + \left|z_j - z_{Alg,j}\right|\right)/NoP \tag{27}$$

$$MAE_{Alg} = \left(\sum_{l=1}^{NoR} MAE_{Alg,l}\right)/NoR \tag{28}$$

The values of the respective tracking algorithms errors were calculated by averaging them for NoR = 100 implementations for different realizations of the measurement process disturbances (Table 2 and 3).

The tables show the cases where the EKF initialization data are correctly selected and the cases of incorrectly chosen values (marked as $EKF_{incorrect}$) which may cause deterioration of location parameters or the inability to determine the location of the object.

Table 2. Averaged error values (m) for trajectories I (T) and various module configurations (C)

	$RMSE_{100}$			MAE_{100}			Profit RMSE		Profit MAE	
Algorithms →	**OLS**	**EKF**	**EKF_{OLS}**	**OLS**	**EKF**	**EKF_{OLS}**	**EKF**	**EKF_{OLS}**	**EKF**	**EKF_{OLS}**
Settings ↓							**versus OLS**			
T 1 C 1	0.27	0.13		0.41	0.27		51.9 %		34.1 %	
T 1 C 2	0.30	0.14		0.44	0.29		53.3 %		34.1 %	
T 1 C 1 $EKF_{incorrect}$	0.27	0.15	0.13	0.41	0.29	0.27	44.5 %	51.9 %	29.3 %	34.1 %
T 1 C 3	0.33	0,15		0.45	0.30		54.5%		33.3 %	

Table 3. Averaged error values (m) for trajectories II (T) and various module configurations (C)

	$RMSE_{100}$			MAE_{100}			Profit RMSE		Profit MAE	
Algorithms →	**OLS**	**EKF**	**EKF_{OLS}**	**OLS**	**EKF**	**EKF_{OLS}**	**EKF**	**EKF_{OLS}**	**EKF**	**EKF_{OLS}**
Settings ↓							**versus OLS**			
T II C 2	0.96	0.25		0.70	0.40		73.9%		42.9 %	
T II C 3	1.72	0.79		0.91	0.53		54.1%		41.7 %	
T II C 3 $EKF_{incorrect}$	1.73	0.77	0.74	0.91	0.55	0.53	55.5%	59.5%	39.6 %	41.8 %
T II C 4	1.01	0.24		0.72	0.38		76.2%		47.2 %	
T II C 4 $EKF_{incorrect}$	0.91	0.24	0.23	0.68	0.39	0.38	73.2%	74.7%	42.6 %	44.1 %

4. CONCLUSIONS

In summary the above considerations, it should be concluded that the use of ultrawideband modules to measure the distances between each of them allow to estimate the position and thus track the trajectory of the air object with a large accuracy.

During the analysis of various types of trajectories, it was found that the accuracy of air object tracking is influenced by both the geospatial configuration of the measuring modules against the tracked object, the type of algorithm used, as well as the accuracy of the initialization data for the EKF algorithm (the initial position of the object).

The trajectory outside the tracking system deployment area increases the error values of the algorithms analysed as well as may lead to their misaction.

Incorrect initialization of the EKF filter may reduce the accuracy of determining the location of the tracked object, and in the extreme case lead to a divergence with the trajectory being analysed.

The modification of the tracking algorithm (using EKF and OLS initialization data) proposed by the authors in some cases enabled the execution of the aircraft tracking process and in others significantly improved accuracy of this process.

Further work will focus on analysing the next algorithms and trying to improve them. In addition, the implementation of the tracking system based on the rules described earlier in real-world conditions will be carried out. The MUT training area will be used for this purpose and the tracked object will be a drone-mounted UWB module (on the octocopter S1000).

REFERENCES

[1] Brown R.G. , Hwang P.Y.C., [Introduction to random signals and applied Kalman filtering]. Wiley, UK, (2012).

[2] Cheung K.W., So H.C., Ma W.K., Chan Y.T., "Least squares algorithms for time-of-arrival-based mobile location", IEEE Transactions on Signal Processing, Volume: 52, Issue: 4 (2004).

[3] Dongchen N., Postolache O. A., Chao M., Meisu Z., Yongshuang W., "UWB Indoor Positioning Application Based on Kalman Filter and 3-D TOA Localization Algorithm", 11th International Symposium on Advanced Topics in Electrical Engineering (ATEE), 28-30 March 2019, Bucharest, Romania, Romania, (2019).

[4] Greene W.H., [Econometric Analysis], Pearson Education, Inc , Prentice Hall, (2011).

[5] Julier S.J., Uhlmann J.K., "A New Extension of the Kalman Filter to Nonlinear Systems". Proc. of AeroSense: The 11th Int. Symp. on Aerospace/Defence Sensing, Simulation and Controls., (1997).

[6] Kaniewski P., Kazubek J. and Kraszewski T., "Application of UWB Modules in Indoor Navigation System". 2017 IEEE International Conference on Microwaves, Antennas, Communications and Electronic Systems (COMCAS), 13-15 November 2017, Tel Aviv, Israel.

[7] Konatowski, S.; Pieniężny, A. T., " A comparison of estimation accuracy by the use of KF, EKF & UKF filters", 13th International Conference on Computational Methods and Experimental Measurements, Prague, Czech Republic, 2007, WIT Transact Modelling & Simulat Computational Methods And Experimental Measurements XIII Book Series: WIT Transactions on Modelling and Simulation, Vol. 46, pp. 779-789, 2007.

[8] Konatowski, S., Sosnowski, B., „Accuracy evaluation of the estimation process by selected non-linear filters", Przeglad Elektrotechniczny, Vol. 87, Issuse 9A, pp. 101-106, 2011.

[9] Kraszewski T., Czopik G., "Tracking of land vehicle motion with the use of distance measurements", Proc. SPIE 11055, XII Conference on Reconnaissance and Electronic Warfare Systems, 110550Y (27 Mar 2019).

[10] Łabowski M., Kaniewski P., Konatowski S., Estimation of Flight Path Deviations for SAR Radar Installed on UAV, Metrology and Measurement Systems, Vol. 23 (2016), No. 3, pp. 383–391, ISSN 0860-8229, DOI: 10.1515/mms-2016-0034.

[11] Matuszewski J., Dikta, A., "Emitter location errors in electronic recognition system," XI Conference on Reconnaissance and Electronic Warfare Systems, Proc. of SPIE - The International Society for Optical Engineering, 10418, art. no. 104180C, pp. C1–C8. DOI: 10.1117/12.2269295, (2017).

[12] Pietrow D., Matuszewski J., Objects detection and recognition system using artificial neural networks and drones, 2017 Signal Processing Symposium (SPSSympo), Jachranka, 14-14.09.2017r., Poland, pp.1-5, DOI: 10.1109/SPS.2017.8053689.

[13] Ravindra S., Jagadeesha S.N., "Time of arrival based localization in wireless sensor networks: a linear approach", Signal & Image Processing : An International Journal (SIPIJ) Vol.4, No.4, August 2013.